

STEADY SEEPAGE IN TRENCHES AND DAMS: EFFECT OF CAPILLARY FLOW

By Michel C. Boufadel,¹ Member, ASCE, Makram T. Suidan,² Member, ASCE,
Albert D. Venosa,³ and Mark T. Bowers,⁴ Member, ASCE

ABSTRACT: Steady seepage from two-dimensional domains is investigated using a dimensionless formulation for variably saturated media that depends on three dimensionless parameters, M , n , and α . The parameter M is the product of the anisotropy ratio and the squared ratio of the vertical length scale to the horizontal length scale. The parameter n increases with the uniformity of the pore sizes, and α represents the ratio of the domain height to the height of the capillary fringe. Our modeling results show that the seepage face height in rectangular domains is always larger than the seepage face height computed from saturated flow models. The results also show that the seepage face height increases with increasing M , increasing n , and/or decreasing α . The outflows computed from the present model are always larger than the outflows computed by the Dupuit assumption. Nomographs for rectangular and trapezoidal domains simulating trenches and dams are presented.

INTRODUCTION

Seepage faces occur commonly in unconfined ground-water flows. Accurate estimation of the seepage face height is important in investigating the stability of porous structures (Freeze and Cherry 1979). Equally important is the computation of the outflow (or discharge) from unconfined domains; outflow values are needed, for example, in the design of constructed wetlands (Sanford et al. 1993).

Dupuit (1863) was the first to present analytical solutions for water table profiles and outflows from long rectangular two-dimensional (2D) domains under steady-state conditions. In obtaining these formulas, two assumptions were made: (1) The flow in the unsaturated zone is negligible; and (2) the vertical component of the flow below the water table is negligible with respect to the horizontal component. Charni (1951) showed that, regardless of the flow distribution below the water table, the Dupuit outflow from rectangular domains is exact provided the unsaturated flow is neglected (Assumption 1). The use of Dupuit's derivation for determining the shape of the free surface in porous media has been less satisfactory because Dupuit did not take into account the existence of a seepage face in his analysis (Muskat 1937). Many analytical and numerical models have been used to compute the seepage face height for saturated media (Assumption 1). Polubarinova-Kochina (1962) presented extensive results in a dimensionless form for various isotropic homogeneous domains under many steady flow conditions. Results for seepage face height from numerical saturated ground-water models have been presented by many workers. A survey of these models was written by Cryer (1976), and a comparison of different methods was published by Craig and Wood (1981). However, many physical situations are encountered where flow occurs in the unsaturated zone. Thus, the seepage face and the outflow results ob-

tained from saturated flow models (analytical and numerical) are limited in application because these models cannot be used to investigate the hydraulics in fine textured media, such as earth dams and constructed wetlands.

Water flow in unsaturated media has been modeled using Richard's equation (Richards 1931). Due to the nonlinearity of Richard's equation, analytical solutions have been obtained for particular cases only (Broabridge and White 1988; Warrick et al. 1991; Basha 1994). Variably saturated numerical models, on the other hand, are able to simulate a wide range of unconfined flow regimes (Freeze 1971; Neuman 1973; Gureghian 1983; Voss 1984; Huyakorn et al. 1986). The effects of the unsaturated flow parameters on the seepage face height and on the outflow from the domain have not been investigated in depth, however. Shamsai and Narasimhan (1991) presented a numerical investigation of steady-state unconfined flows in 2D isotropic rectangular domains. Their results were obtained for isotropic domains and, hence, could not account for anisotropy. Furthermore, the results were reported in a dimensional form, which does not allow extension to other values of unsaturated flow parameters. Boufadel et al. (1998) presented a dimensionless formulation and a finite-element model for 2D variably saturated flow in anisotropic media. In the current manuscript, the formulation and model are used to investigate the effects of the unsaturated zone on seepage face heights and outflows from hypothetical unconfined anisotropic rectangular domains. An application for an earth dam is presented.

GOVERNING EQUATIONS

Neglecting the compressibility of water and the source/sink term, the governing equation for 2D variably saturated flow in porous media written in a dimensionless form is (Boufadel et al. 1998)

$$\phi \frac{\partial S}{\partial t} + S_s S \frac{\partial \psi}{\partial t} = M \frac{\partial}{\partial x} \left(K_x \frac{\partial \psi}{\partial x} \right) + \frac{\partial}{\partial z} \left(K_z \left[\frac{\partial \psi}{\partial z} + 1 \right] \right) \quad (1)$$

where M = dimensionless number given by

$$M = \frac{K_{x0} L_z^2}{K_{z0} L_x^2} \quad (2)$$

and where $K_x = K_x^*/K_{x0}$; $K_z = K_z^*/K_{z0}$; $x = x^*/L_x$; $z = z^*/L_z$; $t = t^*/(L_z^2/K_{z0})$; $S_s = S_s^* L_z$; $\psi = \psi^*/L_z$; and the (*) stands for dimensional quantity. The term ϕ is the porosity (-) [where (-) signifies dimensionless quantity], S is the soil moisture ratio (-) (or relative soil moisture) given by $S = \theta/\phi$ where θ is the water content (-); ψ^* is pressure head (L); S_s^* is the specific storage per unit water weight (L^{-1}), given by $S_s^* = \delta\phi/\delta\psi^*$; and K_x^* and K_z^* are the horizontal and vertical hydraulic con-

¹Dept. of Civ. and Envir. Engrg., Univ. of Cincinnati, Cincinnati, OH 45221; now Res. Asst. Prof., Dept. of Envir. Engrg. and Sci., Clemson Univ., P.O. Box 340919, Clemson, SC 29634-0919; corresponding author. E-mail: mboufad@ces.clemson.edu

²Herman Schneider Prof. of Envir. Engrg., Dept. of Civ. and Envir. Engrg., Univ. of Cincinnati, Cincinnati, OH 45221.

³Microbiologist, U.S. Envir. Protection Agency, Nat. Risk Mgmt. Res. Lab., Cincinnati, OH 45269.

⁴Assoc. Prof., Dept. of Civ. and Envir. Engrg., Univ. of Cincinnati, Cincinnati, OH.

Note. Discussion open until August 1, 1999. To extend the closing date one month, a written request must be filed with the ASCE Manager of Journals. The manuscript for this paper was submitted for review and possible publication on February 3, 1997. This paper is part of the *Journal of Hydraulic Engineering*, Vol. 125, No. 3, March, 1999. ©ASCE, ISSN 0733-9429/99/0003-0286-0294/\$8.00 + \$.50 per page. Paper No. 15051.

ductivities, respectively, and they are assumed to be parallel to the major axes of anisotropy. The subscript 0 represents the saturated hydraulic conductivities.

The soil moisture and the hydraulic conductivity are correlated experimentally to the pressure head by the van Genuchten model (1980), which is written in a dimensionless form as (Boufadel et al. 1988)

$$\text{for } \psi \geq 0.0 \quad K_x = K_z = 1.0 \quad (3a)$$

For $\psi < 0.0$:

$$S_e = \frac{S - S_r}{1 - S_r} = \left[\frac{1}{1 + (\alpha|\psi|)^n} \right]^m \quad (3b)$$

$$K_j = S_e^{(1/2)} [1 - (1 - S_e^{1/m})^m]^2 \quad (3c)$$

where $j = (x, z)$; $m = 1 - 1/n$; and $\alpha = \alpha^* L_z$. The parameter α^* represents a characteristic pore size, and higher α^* values imply a coarser material. The inverse of α^* provides an estimate of the capillary fringe (zone of considerable moisture) (Bear 1972). The term n represents the uniformity of the porous medium with higher values of n implying a more uniform pore space distribution (van Genuchten 1980; Wise et al. 1994).

Under steady-state conditions, all of the terms associated with the temporal derivative in (1) vanish; the effective saturation ratio is computed directly from the second equality in (3b), which depends solely on n , α , and ψ . Hence, ϕ , S_s , and S_r values need not be considered in the remainder of this manuscript. Only M , n , and α are needed. The dimensionless number M combines the effects of anisotropy and the aspect ratio of the porous medium. The dimensionless number α represents the ratio of the domain height L_z to the thickness of the capillary fringe $1/\alpha^*$.

MODEL IMPLEMENTATION

The numerical model developed by Boufadel et al. (1998) is a Galerkin finite-element model for 2D flows in variably saturated anisotropic media. Time integration is done using the modified Picard method with mass lumping (Celia et al. 1990), and triangular finite elements are used for spatial discretization (Huyakorn and Pinder 1983). At each Picard iteration, the resulting system of linear equations is solved using a standard band Choleski decomposition method (Najem 1982; Istok 1989). Details of the modeling approach, model verification,

and model validation are given by Boufadel (1998) and Boufadel et al. (1998).

APPLICATIONS

Seepage Face Boundary

A seepage face is an external boundary of the saturated zone where water leaves the soil and the pressure head ψ is uniformly zero. The height of the seepage face is generally not known a priori and is determined iteratively. Following Neuman (1973) and Pinder and Gray (1977), the location of the seepage face is first estimated then updated as follows: At all nodes with $\psi < 0$, a Neuman-type boundary is specified with the inwardly directed normal Darcy flux q set to zero. The final solution should provide negative values of q at nodes where the pressure is prescribed as zero (i.e., outward flow) and negative values of ψ at nodes where q is prescribed as zero. More information is found in Neuman (1973) and Cooley (1983). The location of the seepage face requires a check on the Darcy flux, which is computed usually by taking the derivatives (numerically) of the computed pressure head over each element. In this work, the Darcy fluxes are computed according to the method presented by Yeh (1981) because this method achieves continuity of the Darcy flux across element boundaries. The normal flux to the seepage face is computed subsequently.

Steady-State Seepage through Rectangular Domain

This example concerns the development of a seepage face at the outlet of a rectangular domain under steady-state flow conditions. The dimensionless domain is a square of dimensionless side lengths equal to 1.0. The boundary condition on the whole left side of the domain is $\psi(x=0, z) = z$ (hydrostatic), and on the right side of the domain $\psi(x=1, z=0) = 0$ (no tailwater). The nodal spacing in both x - and z -directions is $\Delta x = \Delta z = 0.01$, forming a mesh of 10,201 nodes and 20,000 triangular finite elements. The fine mesh is intended to reduce discretization errors in the computation of the seepage face height and the outflow. Since steady-state results are sought, the model was run in the transient regime with increasing time steps until no variation in the solution was observed (i.e., convergence).

Seepage Face Height

Results for various values of M and (α, n) pairs are plotted in Fig. 1. The α values were chosen to represent two situa-

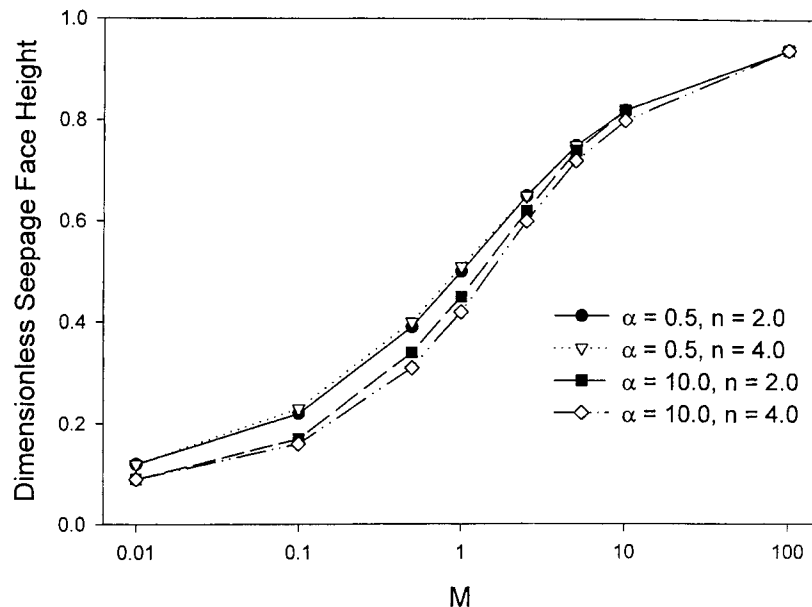


FIG. 1. Variation of Seepage Face Height from Rectangular Domains as Function of M for Four (α, n) Pairs

$M = 1.0; n = 4.0$

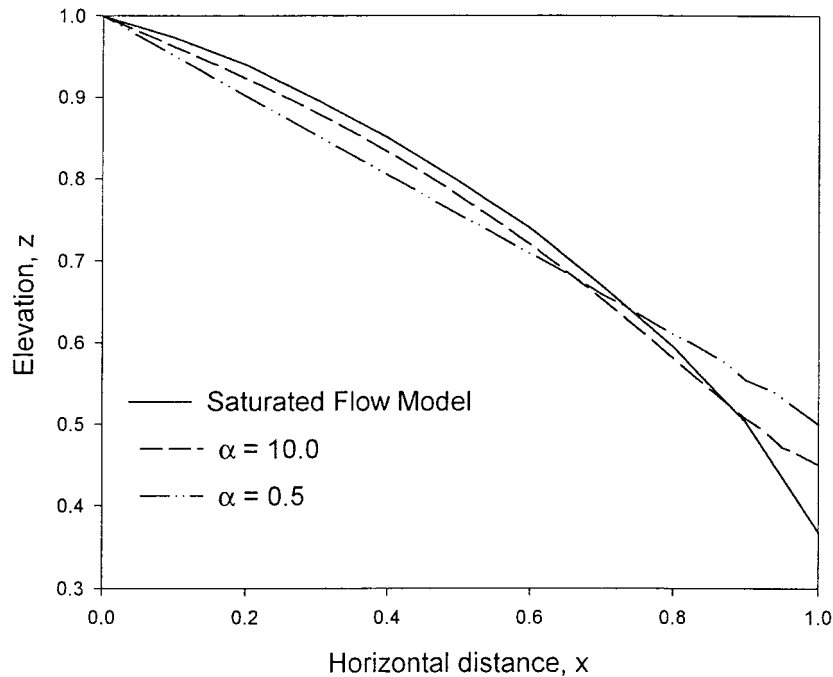


FIG. 2. Effects of α on Water Table Profile and Comparison with Water Table Profile Obtained from Saturated Flow Model (Hornung and Krueger 1985)

tions: $\alpha = 10.0$ represents a case where the capillary fringe is $\sim 10\%$ of the height of the domain, whereas $\alpha = 0.5$ was chosen to represent a situation where the capillary fringe extends to the top of the domain. The n values were selected in the intermediate range of the values reported in the literature (van Genuchten 1980; Morell-Seytoux et al. 1996).

As seen in Fig. 1, the location of the seepage face is much more sensitive to the parameter M than to the unsaturated-flow parameters. Large M values correspond to a large ratio of the vertical dimension to the horizontal dimension or to high anisotropy ratio (defined as K_{x0}/K_{z0}). In both cases, the water table would reach the exit wall of the domain without a considerable drop in height. Conversely, when M was decreased, the seepage face height dropped. These results are consistent with observations by Shamsai and Narasimhan (1991) for a rectangular isotropic domain.

As seen in Fig. 1, the effect of the unsaturated-flow parameters (α, n) on the seepage face height is small at the extrema of M , especially at $M = 100$. However, marked differences in the seepage height are observed at intermediate values of M (≈ 1.0). Fig. 1 shows, as expected, that the seepage face height decreases with increasing α . Fig. 2 shows the water table (or phreatic surface) in the domain for $M = 1.0, n = 4.0$, and two values of α . It also shows the water table profile as obtained from Hornung and Krueger (1985), which was based on the Polubarinova-Kochina (1962) approach (saturated flow model). For both α values, the seepage face height obtained from the present model was larger than the one obtained from the saturated-flow model (Hornung and Krueger 1985). Shamsai and Narasimhan (1991) reported a similar observation in isotropic media. For a large α value, the water table profile from the present model approached the water table profile of the saturated flow model. However, as α decreases, capillary forces increase, and because they have their major effects in the vertical direction (upward), the seepage face height increases. Hence, the seepage face height obtained by including the contribution of the unsaturated zone will always be larger than the one obtained from the saturated flow model.

The effect of n on seepage face height is minor when com-

pared to the effects of M and α (Fig. 1), which shows that the dimensionless formulation is adequate for investigating a wide range of seepage problems. This is because the parameter n is an intrinsic property of the medium whereas M and α can be obtained for any type of soils.

Contribution of Unsaturated Zone to Outflow

The dimensionless inflows and outflows from the domain were computed by integrating the horizontal dimensionless Darcy flux, $q_x = K_x \delta\psi/\delta x$, along the left boundary and the seepage face height, respectively. The maximum difference between inflows and outflows was $< 1\%$ in most cases and $< 3\%$ for $M = 0.01$. The errors in mass balance occurred most likely in the Darcy flux computation at the exit boundary of the domain due to high pressure head gradients. Fig. 3 shows the dimensionless outflow from the domain for the previous values of M, α , and n .

All of the dimensionless outflow values are > 0.5 , which corresponds to the dimensionless outflow computed by assuming saturated flow only (Charni 1951)

$$Q_{\text{Charni}} = \frac{(\xi_{\text{Inflow}}^2 - \xi_{\text{Outflow}}^2)}{2L} = \frac{(1.0^2 - 0.0^2)}{(2)(1.0)} = 0.50 \quad (4)$$

where ξ = total head given by $\xi = \psi + z$. Eq. (4) can be obtained using the Dupuit assumption (Bear 1972). Shamsai and Narasimhan (1991) reported that the outflow computed using their variably saturated model was in some cases $\sim 25\%$ more than the outflow computed by (4).

The total horizontal flow at a section x , at steady state, is given as follows:

$$Q(x) = Q = \int_0^H q_x dz = \int_0^{h(x)} q_x dz + \int_{h(x)}^H q_x dz \quad (5)$$

where the fact that $Q(x)$ is uniform with respect to x is explicitly shown. H is the height of the domain (constant herein). The first term on the right-hand side represents the flow in the saturated zone while the second term represents the flow in

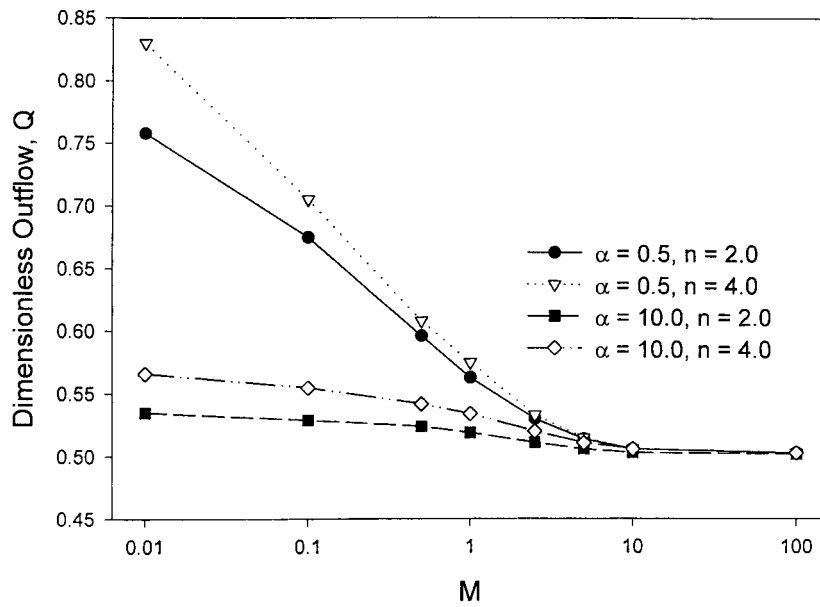


FIG. 3. Variation of Outflow from Rectangular Domain as Function of M for Four (α, n) Pairs

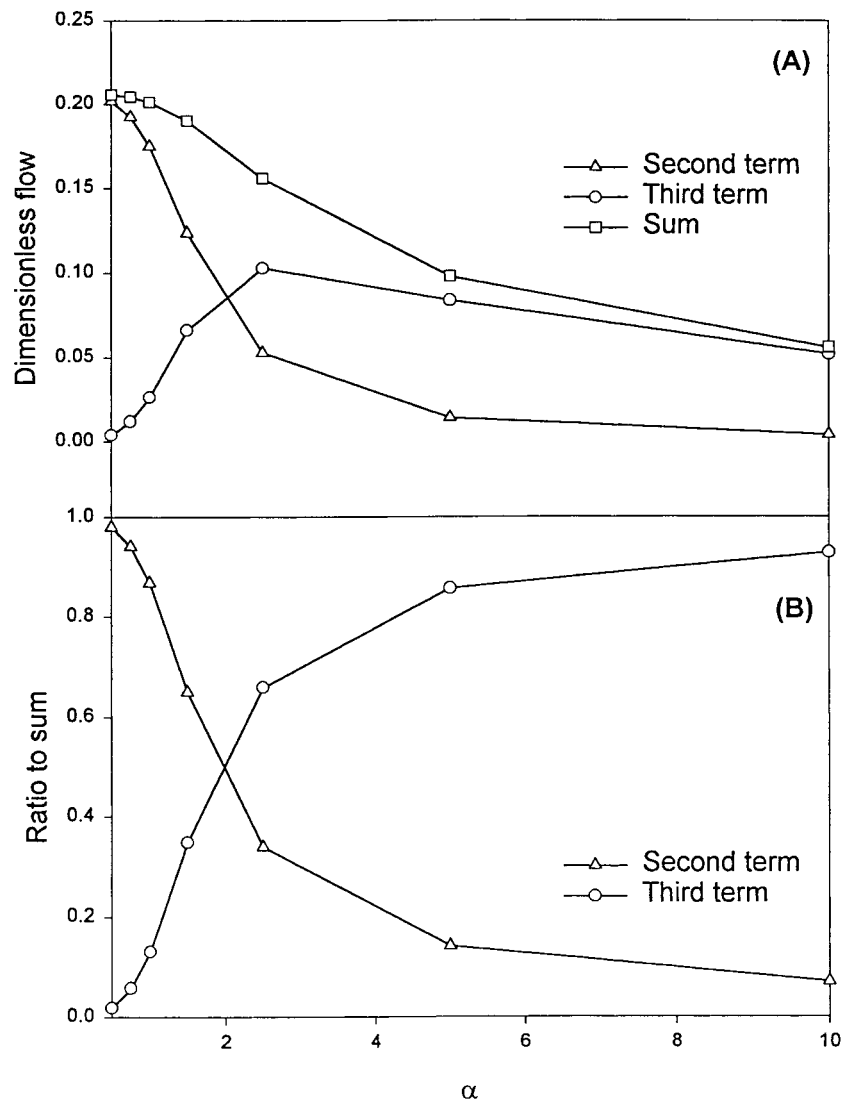


FIG. 4. Variation of Second and Third Terms in Eq. (10) and Their Sum as Function of α for $M = 0.1$ and $n = 4.0$

the unsaturated zone. Thus, the total flow across every section x is the sum of the flow occurring in the saturated and unsaturated zones, namely

$$Q = Q_{sat}(x) + Q_{uns}(x) \quad (6)$$

Notice that Q_{sat} is generally different from Q_{Charni} ; it is only the horizontal flow under the water table at section x and can thus vary with x , whereas Q_{Charni} is uniform with respect to x . The total outflow from the rectangular domain can now be written (see Appendix I)

$$Q = K_0 \frac{H^2}{2L} - \frac{1}{L} \int_{h_s}^H K \psi dz + \int_0^L \left[\int_{h_s}^H \psi \frac{\partial K}{\partial x} dz \right] dx \quad (7)$$

The first term on the right-hand side is the outflow Q_{Charni} . The term h_s is the seepage face height. Both the second and the third terms are positive (because ψ and $\delta K/\delta x$ are negative above the water table). Hence, the contribution of the unsaturated zone is to increase the outflow from the domain. The second term depends on the pressure head distribution (in the unsaturated zone) at the exit face of the domain only, whereas the third term depends on the pressure field in the whole unsaturated zone.

The contribution of the second and the third terms to the outflow from the domain varied significantly with the parameter α . Fig. 4(a) shows, for $M = 0.1$ and $n = 4$, the variation of the second and third term and their sums as a function of α . Fig. 4(a) shows that the total unsaturated flow decreased with α . It also shows that the second term of (7) decreased rapidly and almost linearly for $0.5 < \alpha < 2.5$ and continued decreasing afterward at a gentler rate. The third term, however, did not vary in a monotonic fashion with α . It increased for $\alpha < 2.5$ and decreased linearly afterwards. This behavior can be explained based on the height of the capillary fringe. For small values of α the capillary fringe is large and the unsaturated hydraulic conductivity K in the domain is very close to its maximum value given by the saturated hydraulic conductivity K_0 (van Genuchten 1980; Boufadel et al. 1998). Although K is large, its variation is small thereby rendering the third term small. However, the second term depends directly on K and not on its variation; hence, it increases with K (i.e., for small α values). For large α values, the capillary fringe is small. Hence,

the second term is small because large values of K are associated with a near-zero pressure head. The third term decreases for very large α values because K is then near zero; hence, its variation is very small. It is only at intermediate α values ($\alpha \approx 2.0$) that the third term reaches its maximum.

Fig. 4(b) shows the variation of the ratio of the second and the third terms to their sum (which varies with α) as a function of α . At small values of α , the major contribution to the unsaturated flow comes from the second term in (7), whereas for $\alpha \geq 2.5$, the major contribution comes from the third term.

In Fig. 3, for a constant (α, n), the outflow approached the value of 0.5 with increasing M that is contrary to the underlying assumptions of (4). This interesting paradox is explained by noticing that in (7), the contribution of the unsaturated flow increases with the difference between H and h_s , which increases with a decreasing M . Therefore, it is concluded that (4) underpredicts greatly the outflow from long rectangular domains.

Although the effect of n on the total outflow is minor in comparison to the effects of M and α (Fig. 3), an explanation is readily available. Decreasing n results in an increase in the density of pores that are too small to allow passage of water through them (Wise et al. 1994). Thus, although a large amount of water is retained in the unsaturated zone, the unsaturated flow is small because most of the water is immobile in that zone.

Linear Pressure Profile

Eq. (7) requires knowledge of the pressure head field in the unsaturated zone, which can be accurately obtained only from a variably saturated numerical model. Here, following Li et al. (1997) the outflow resulting from assuming that the pressure head varies linearly with elevation (hydrostatic) in the capillary fringe is investigated. The quantities $h(x)$ and $\delta\psi/\delta x$ in the third term of (7) require knowledge of the pressure head variation in the horizontal direction that is assumed to be linear. Thus, the water table is assumed to vary linearly from H to h_s and $\delta\psi/\delta x = -(H - h_s)$, an assumption that does not affect the second term in (7). The hydraulic conductivity is computed from (3) after substituting the elevation above the capillary zone to the pressure head ψ . The seepage face height h_s (Fig. 1) is assumed to be found accurately from the analytical solution that assumed

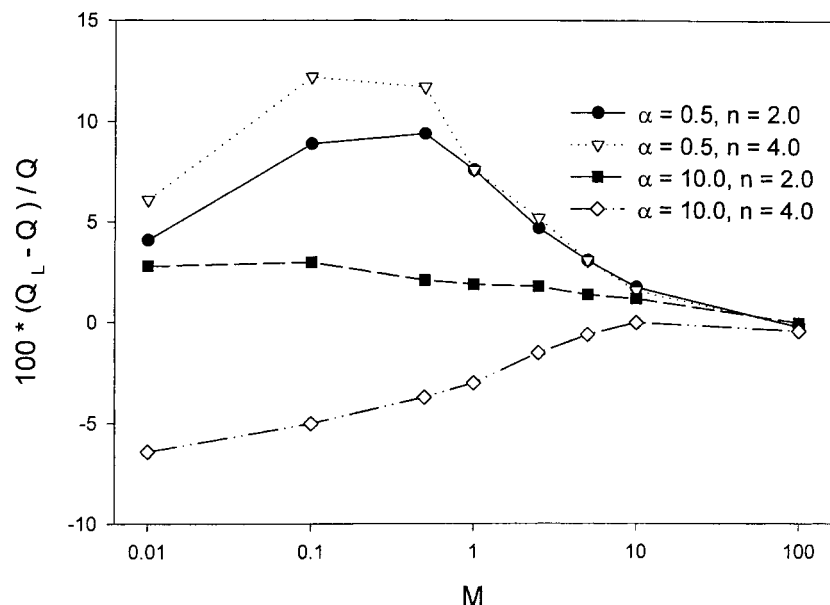


FIG. 5. Variation of Percent Difference between Total Outflow Computed under Linear Pressure Distribution Assumption, Q_L , and Outflow Given by Present Model, Q

a hydrostatic pressure distribution in the capillary fringe. The hydraulic conductivity is computed from (3) after substituting the elevation above the capillary zone to the pressure head ψ . Numerical integration of q_x was performed from the water table to the minimum of H and $(h + 1/\alpha)$.

Fig. 5 shows the relatively small difference between the outflows computed under the linear pressure distribution assumption Q_L and the outflows computed from the numerical model Q in Fig. 3. The largest difference ($\sim 12\%$) occurred for $0.1 < M < 1.0$, whereas the difference for $M \geq 2.5$ was $\leq 5\%$. The difference between Q_L and Q , for $\alpha = 10.0$, increased (in absolute value) with decreasing M and started to level off at low M values (note the logarithmic scale). However, a different behavior was observed for $\alpha = 0.5$; the difference between Q_L and Q increased with decreasing M until $M = 0.1$ for $n = 0.4$ ($M = 0.5$ for $n = 2.0$) and then decreased for $M = 0.01$. For both α values, the outflow Q_L depended greatly on the unsaturated characteristics of the soil, especially at low M values. For $\alpha = 0.5$, Q_L overpredicted the correct outflow Q , whereas two situations were observed for $\alpha = 10.0$; Q_L overpredicted Q for $n = 2.0$ and underpredicted it for $n = 4.0$. However, the difference between Q_L and Q for $\alpha = 10$ was generally smaller than the one for $\alpha = 0.5$. Therefore, it is concluded that the linear profile approximation tends to provide a better estimate for the outflow for a system with a small capillary fringe than for a system where the capillary fringe is affected by the upper (impermeable) boundary of the domain. For $\alpha = 0.5$, the effect of the top boundary decreases at $M = 0.01$ due to a reduction in the seepage face height. At large M values the effect of the top boundary on the flow distribution is large but the unsaturated flow is small. It is only at intermediate values of M that Q_L deviates greatly from Q . For both $\alpha = 0.5$ and $\alpha = 10$, Q_L at $n = 2$ agreed more closely with Q . It may be concluded that the linear pressure profile distribution assumptions are more valid for soils with a relatively wide pore-size distribution.

Variation of Unsaturated Flow

Eq. (7) provides only the outflow from the domain (i.e., the flow at $x = L$) and does not show clearly the interaction between the saturated and the unsaturated zones within the domain. By considering the second term in (10) and using the integral mean value theorem (Atkinson 1978) one can write

$$Q_{uns}(x) = - \int_h^H K \frac{\partial \psi}{\partial x} dz = \left(- \frac{\partial \psi}{\partial x} \right)_{ave} \int_h^H K dz \quad (8)$$

Thus, $Q_{uns}(x)$ is positive being the product of two positive terms. At $x = 0$, $Q_{uns}(0) = 0$ because $h = H$ and the integral is zero, whereas at $x = L$, the gradient $(-\partial\psi/\partial x)_{ave}$ is zero (no flow boundary) rendering $Q_{uns}(L) = 0$. Thus, Q_{uns} is a positive quantity that equals zero at both $x = 0$ and $x = L$, which indicates that it must pass through one maximum (at least) between these two points. This implies, when considering (6), that Q_{sat} has a minimum at the same location because the total horizontal flow Q is uniform at steady state. Fig. 6(a) shows for $M = 0.1$, $\alpha = 0.5$, and $n = 4$ what the present analysis predicted; Q_{uns} increased from 0.0 to 0.34 at $x = 0.79$ and then decreased to near zero (0.008) at the outlet. Q_{sat} showed the converse behavior with a minimum value of 0.36 at $x = 0.79$. Thus, for small M values, the horizontal unsaturated flow can be $\sim 100\%$ of the horizontal saturated flow in the domain. For $M = 10$, $\alpha = 0.5$, and $n = 4$, Fig. 6(b) shows that the contribution of the unsaturated flow to the total horizontal flow is negligible. The maximum value of Q_{uns} , 0.015, is $\sim 2\%$ of the minimum saturated flow Q_{sat} , 0.495. Notice that the error in the total outflow takes place only at the seepage face of the

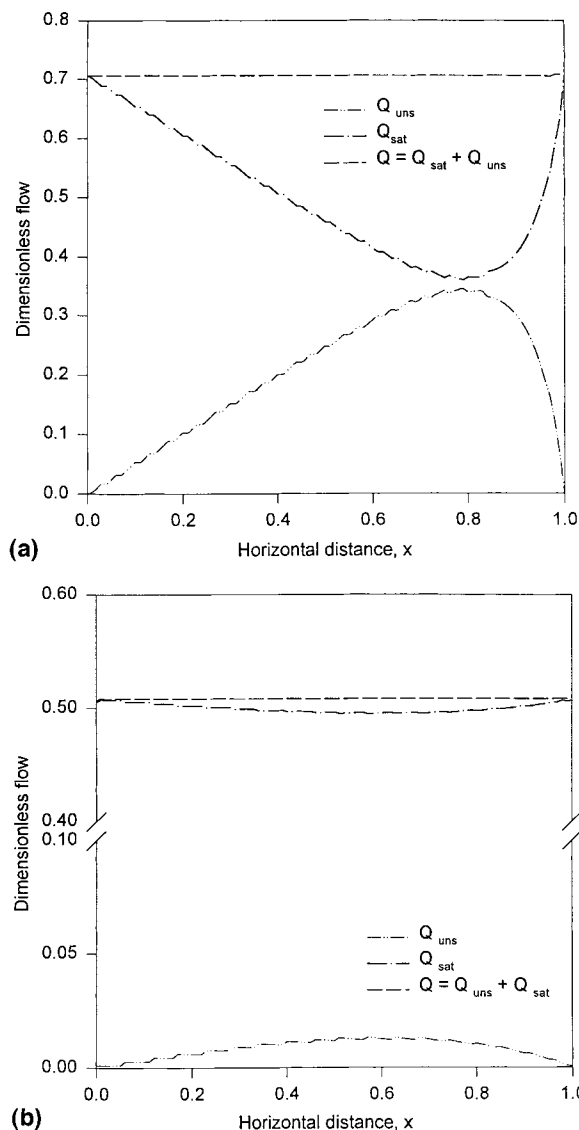


FIG. 6. Distribution and Magnitude of Unsaturated and Saturated Flows as Functions of x for ($\alpha = 0.5$, $n = 4.0$) and for: (a) $M = 0.1$; (b) $M = 10.0$

domain due to high pressure gradients as seen in the small “jump” around $x = 1.0$ in Figs. 6(a and b).

Dimensional Outflow

The dimensional outflow from the domain can be written as

$$Q^* = K_{z0} L_x M Q \quad (9)$$

where Q = dimensionless outflow of the domain given in Fig. 3. Eq. (9) provides an explanation for the numerical observation of Shamsai and Narasimhan (1991) that the outflow from the isotropic domain ($L_x = 3.0$ m, $L_z = 2.0$ m) adopted from Vaucelin et al. (1979) was almost proportional to the saturated hydraulic conductivity. The M value of that system is ~ 0.5 , which results in a maximum variation of the outflow with unsaturated parameters of $< 8\%$ (Fig. 3). The effect of this variation on the dimensional outflow is overshadowed by large changes in the saturated isotropic hydraulic conductivity. Notice that the values of the hydraulic conductivities do not affect the dimensionless outflow Q ; it is rather their ratio that appears in the governing equation (1). Thus, the variation of the dimensional outflow is almost proportional to the

variation of the saturated isotropic hydraulic conductivity. Eq. (9) shows that the quasi-proportionality of the total outflow to the saturated hydraulic conductivity exists in anisotropic media provided the ratio of anisotropy (hence M) is conserved.

The practical aspect of the present analysis of seepage problems in rectangular domains is seen in the nomographs in Figs. 1 and 3. The ranges of M , α , and n were intended for most man-made systems such as constructed trenches and constructed wetlands. For intermediate values, linear interpolation between existing values can be used.

Steady-State Seepage through Dam

Under a steady-state regime, failures of an earth dam can result from excessive seepage, from piping at the toe, or from slope failures on the dam faces. Many textbooks provide design features to reduce the probability of failure (Cedergren 1967; Spangler and Handy, 1982). In most cases, the solution results in a reduction of the seepage face height by lowering the highest exit point at the downstream face of the dam (Freeze and Cherry 1979). For this reason, a nomograph is presented herein for seepage face height for a typical dam on an impermeable stratum as shown in Fig. 7. The geometry of the domain was selected to represent average-sized dams because the crest width is 20% of the base of the dam, which would be large for larger dams (Cedergren 1967). Fig. 8 shows seepage face heights for a wide range of M . The large values

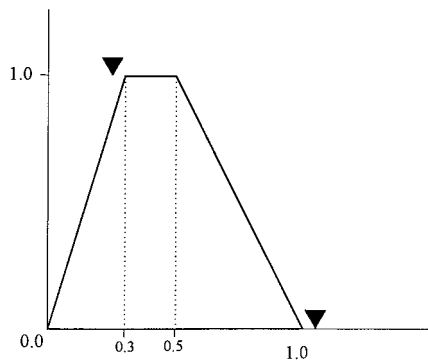


FIG. 7. Geometry and Boundary Conditions of Trapezoidal Dam

of M do not necessarily result from the aspect ratio L_z/L_x , which is dictated by stability requirements; they can result from anisotropy due to compaction (Cedergren 1967). The variation of the seepage face height with α and n at large M is similar to the rectangular section. However, the seepage face height increased at smaller values of M , which is due to the sloping downstream face of the dam. This is because small values of M result in water flowing more freely in the horizontal direction than downward, toward the narrow end of the dam. The value $M \approx 0.05$ provided the most economical solution because it resulted in the smallest seepage height. A complete set of nomographs for dams of various geometry is not presented here for brevity.

SUMMARY AND CONCLUSIONS

Seepage problems were investigated using a dimensionless formulation for water flow in 2D variably saturated anisotropic media. The dimensionless formulation depended on three dimensionless parameters, M , n , and α . M is the product of the anisotropy ratio and the squared ratio of the vertical length scale to the horizontal length scale. The parameter n represents the pore size distribution and α represents the ratio of the vertical length of the domain to the height of capillary fringe. The nondimensionalization is not limited to the van Genuchten model, and it can be used with other capillary-retention models provided they are dimensionally homogeneous [such as the Gardner (1958) model]. If this is not the case, an empirical correlation similar to the work of Morell-Seytoux et al. (1996) should be obtained between such models and the van Genuchten model. For a rectangular domain, the seepage face height decreased with decreasing M , decreasing n , and/or increasing α . The dimensionless outflow increased with decreasing M , increasing n , and/or decreasing α . Within the domain, the unsaturated flow reached 100% of the saturated flow at low M values. The dimensionless outflows Q_L , computed by assuming a linear pressure variation in the horizontal direction and a hydrostatic pressure profile in the capillary fringe, agreed more closely with the outflows computed from the present numerical model at large α values than at small α values. Nomographs for rectangular domains and trapezoidal dams were presented. For trapezoidal domains, the seepage face height decreased first with decreasing M and increased later at low values of M . This allowed the selection of the most economical aspect ratio of a hypothetical dam.

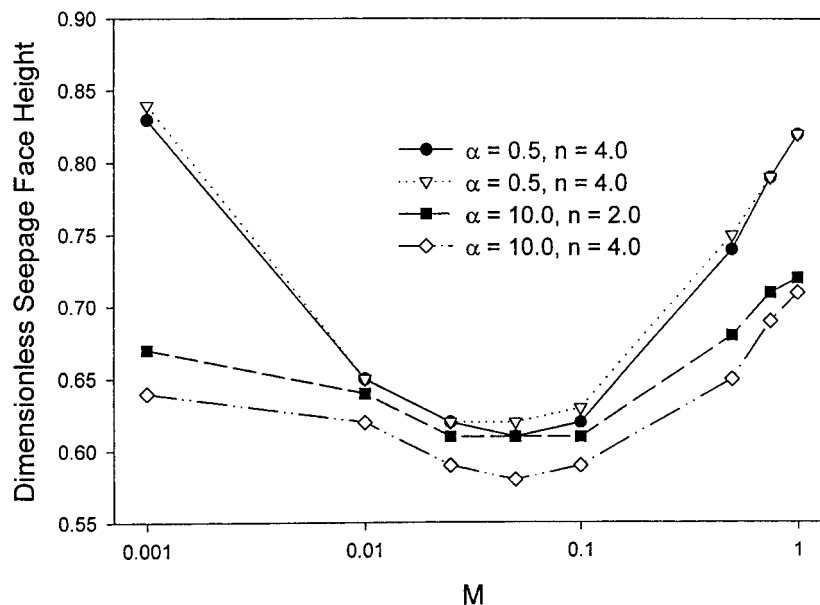


FIG. 8. Dimensionless Seepage Face Height for Trapezoidal Domain as Function of M for Four (α, n) Pairs

APPENDIX I

By applying Darcy's law, (6) is rewritten

$$Q = - \int_0^h K \frac{\partial \psi}{\partial x} dz - \int_h^H K \frac{\partial \psi}{\partial x} dz \quad (10)$$

where the dependence of h on x is not shown explicitly. Using integration by parts on the second term on the right-hand side of (10), one obtains the following:

$$Q_{ms}(x) = - \int_h^H K \frac{\partial \psi}{\partial x} dz = - \int_h^H \frac{\partial}{\partial x} (K\psi) dz + \int_h^H \psi \frac{\partial K}{\partial x} dz \quad (11)$$

By the Leibnitz rule (Dean and Dalrymple 1984)

$$\begin{aligned} \frac{\partial}{\partial x} \int_h^H K\psi dz &= \int_h^H \frac{\partial}{\partial x} (K\psi) dz + K(x, H)\psi(x, H) \frac{\partial H}{\partial x} \\ &- K(x, h)\psi(x, h) \frac{\partial h}{\partial x} \end{aligned} \quad (12)$$

The second term is equal to zero because H does not vary with x , and the third term is identically equal to zero because the pressure $\psi(x, h)$ is zero at the water table by definition. Thus, (10) is rewritten

$$Q = -K_0 \int_0^h \frac{\partial \psi}{\partial x} dz - \frac{\partial}{\partial x} \int_h^H \psi K dz + \int_h^H \psi \frac{\partial K}{\partial x} dz \quad (13)$$

where K_0 being a constant is taken out of the first integral. Multiplying both sides of (13) by dx and integrating from $x = 0$ to $x = L$, one obtains

$$\begin{aligned} Q \int_0^L dx &= -K_0 \left[\int_0^h \xi dz - \frac{h^2}{2} \right]_0^L - \left[\int_h^H \psi K dz \right]_0^L \\ &+ \int_0^L \left[\int_h^H \psi \frac{\partial K}{\partial x} dz \right] dx \end{aligned} \quad (14)$$

Notice that Q is outside of the integral because it is a constant; $Q =$ horizontal flow in the whole domain and not only in the saturated zone as assumed by (4). The details of the computation of the first term are shown in Bear (1972); hence, only the final result will be shown here. The second term becomes

$$- \left[\int_h^H \psi K dz \right]_0^L = - \int_{h(L)}^{H(L)} \psi K dz + \int_{h(0)}^{H(0)} \psi K dz \quad (15)$$

The second term on the right-hand side is equal to zero because $h(0) = H$. Using the result of (15) and dividing both sides of (14) by L , (7) is obtained.

ACKNOWLEDGMENTS

This work was supported, in part, by the U.S. Environmental Protection Agency's National Risk Management Research Laboratory, Cincinnati, Ohio, under Cooperative Agreement No. CR-821029. However, it does not necessarily reflect the views of the Agency, and no official endorsement should be inferred.

APPENDIX II. REFERENCES

- Atkinson, K. E. (1978). *An introduction to numerical analysis*. Wiley, New York, 587.
- Basha, H. A. (1994). "Multidimensional steady infiltration with prescribed boundary conditions at the soil surface." *Water Resour. Res.*, 30, 2105–2118.
- Bear, J. (1972). *Dynamics of fluids in porous media*. Elsevier Science, New York.
- Boufadel, M. C. (1988). "Nutrient transport in beaches: Effect of tides, waves, and buoyancy." PhD thesis, Dept. of Civ. and Envir. Engrg., University of Cincinnati, Cincinnati.
- Boufadel, M. C., Suidan, M. T., Venosa, A. D., Rauch, C. H., and Biswas,

- P. (1998). "2D variably saturated flows: Physical scaling and Bayesian estimation." *J. Hydrologic Engrg.*, ASCE, 3(4), 223–231.
- Broabridge, P., and White, I. (1988). "Constant rate rainfall infiltration, a versatile nonlinear model. Part 1: Analytical solution." *Water Resour. Res.*, 24, 145–154.
- Cedergren, H. R. (1967). *Seepage, drainage, and flow nets*. Wiley, New York, 489.
- Celia, M. A., Bouloutas, E. T., and Zarba, R. L. (1990). "A general mass-conservative numerical solution for the unsaturated flow equation." *Water Resour. Res.*, 26, 1483–1496.
- Charni, I. A. (1951). A rigorous derivation of Dupuit's formula for unconfined seepage with seepage surface, *Doklady Akademii Nauk USSR*, 6, 79 (in Russian).
- Cooley, R. L. (1983). "Some new procedures for numerical solution of variably saturated flow problems." *Water Resour. Res.*, 19, 1271–1285.
- Craig, A. W., and Wood, W. L. (1981). "Cost-efficiency study of various methods for solving the seepage through dam problem using variational inequalities." *Int. J. Numer. Methods in Engrg.*, 17, 1325–1333.
- Cryer, C. W. (1976). "A survey of steady-state porous flow free boundary problems." *MRC Tech. Sum. Rep. 1657*, Madison Research Center, Madison, Wisconsin.
- Dean, R. G., and Dalrymple, R. A. (1984). *Water wave mechanics for engineers and scientists*. Prentice-Hall, Englewood Cliffs, N.J., 353.
- Dupuit, J. (1863). *Etudes theoriques et pratiques sur le mouvement des eaux dans les canaux decouverts et a travers les terrains permeables*, 2nd Ed., Dunod, Paris, (in French).
- Freeze, R. A. (1971). "Three-dimensional, transient, saturated-unsaturated flow in a groundwater basin." *Water Resour. Res.*, 7(2), 347–366.
- Freeze, R. A., and Cherry, J. A. (1979). *Groundwater*. Prentice-Hall, Englewood Cliffs, N.J., 604.
- Gardner, W. R. (1958). "Some steady state solutions of the unsaturated moisture flow equation with application to evaporation from a water table." *Soil Sci.*, 4, 85, 228–232.
- Gureghian, A. B. (1983). "TRIPM: A two-dimensional finite-element model for the simultaneous transport of water and reacting solutes through saturated and unsaturated porous media." *Tech. Rep.*, Batelle Memorial Institute, Columbus, Ohio.
- Hornung, U., and Krueger, T. (1985). "Evaluation of the Polubarinova-Kochina formula for the dam problem." *Water Resour. Res.*, 21, 395–398.
- Huyakorn, P. S., and Pinder, G. F. (1983). *Computational methods in subsurface flow*. Academic, New York, 473.
- Huyakorn, P. S., Springer, E. P., Guvanenas, V., and Wadsworth, T. D. (1986). "A three-dimensional finite element model for simulating water flow in variably saturated porous media." *Water Resour. Res.*, 22, 1790–1808.
- Istok, J. (1989). *Groundwater modeling by the finite element method*. American Geophysical Union, Washington, D.C.
- Li, L., Barry, D. A., Parlange, J.-Y., and Pattiaratchi, C. B. (1997). "Beach water table fluctuations due to wave run-up: Capillarity effects." *Water Resour. Res.*, 33(5), 935–945.
- Morell-Seytoux, H. J., Meyer, P. D., Nacache, M., Touma, J., van Genuchten, M. T., and Lenhard, R. J. (1996). "Parameter equivalence for the Brooks-Corey and van Genuchten soil characteristics: Preserving the effective capillary drive." *Water Resour. Res.*, 32(5), 1251–1258.
- Muskat, M. (1937). *The flow of homogeneous fluids through porous media*. McGraw-Hill, New York, 763.
- Najem, W. (1982). *Introduction aux techniques du calcul numerique*, Engrg. Facu., University of Saint Joseph, Beirut, Lebanon, 54 (in French).
- Neuman, S. P. (1973). "Saturated-unsaturated seepage by finite elements." *J. Hydr. Div.*, ASCE, (12), 2233–2250.
- Pinder, G. F., and Gray, W. G. (1977). *Finite element simulation in surface and subsurface hydrology*. Academic, New York, 294.
- Polubarinova-Kochina, P. Ya. (1963). *Theory of ground water movement*. Translated from Russian by J. M. R. De Wiest, Princeton University Press, Princeton, N.J., 613.
- Richards, L. A. (1931). "Capillary conduction of liquids through porous mediums." *Phys.*, 1, 318–333.
- Sanford, W. E., Parlange, J.-Y., and Steenhuis, T. S. (1993). "Hillslope drainage with sudden drawdown: Closed form solution and laboratory experiment." *Water Resour. Res.*, 29(7), 2313–2321.
- Shamsai, A., and Narasimhan, T. N. (1991). "A numerical investigation of free surface-seepage face relationship under steady state flow conditions." *Water Resour. Res.*, 27(3), 409–421.
- Spangler, M. G., and Handy, R. L. (1982). *Soil engineering*. Harper and Row, New York, 819.
- van Genuchten, M. Th. (1980). "A closed-form equation for predicting

the hydraulic conductivity of unsaturated soils." *Soil Sci. Soc. Am. Proc.*, 44, 892–898.

- Vauclin, M., Khanji, D., and Vachaud, G. (1979). "Experimental and numerical study of a transient, two-dimensional unsaturated-saturated water table recharge problem." *Water Resour. Res.*, 15(5), 1089–1101.
- Verma, R. D., and Brutsaert, W. (1970). "Unconfined aquifer seepage by capillary flow theory." *J. Hydr. Div.*, ASCE, 96(6), 1331–1344.
- Voss, C. I. (1984). "SUTRA, a finite-element model for saturated-unsaturated. Fluid-density-dependent groundwater flow with energy transport or chemically reactive single species solute transport." *Water Resour. Invest. Rep. 84-4369*, U.S. Geological Survey.
- Warrick, A. W., Islas, A., and Lomen, D. O. (1991). "An analytical solution to Richard's equation for time varying infiltration." *Water Resour. Res.*, 27(5), 763–766.
- Wise, W. R., Clement, T. P., and Molz, F. J. (1994). "Variably saturated modeling of transient drainage: Sensitivity to soil properties." *J. Hydro.*, Amsterdam, 161, 91–108.
- Yeh, G. T. (1981). "On the computation of Darcian velocity and mass balance in the finite element modeling of groundwater flow." *Water Resour. Res.*, 17, 5, 1529–1534.

APPENDIX III. NOTATION

The following symbols are used in this paper:

- h = height of water table from impermeable stratum;
 h_s = height of seepage face from impermeable stratum;
 K = hydraulic conductivity for isotropic domains;

- K_x = horizontal hydraulic conductivity;
 K_z = vertical hydraulic conductivity;
 K_{x0} = saturated horizontal hydraulic conductivity for anisotropic domains;
 K_{z0} = saturated vertical hydraulic conductivity for anisotropic domains;
 K_0 = saturated hydraulic conductivity for isotropic domains;
 L or L_x = horizontal length of domain;
 L_z or H = vertical length of domain;
 M = product of anisotropy ratio and squared ratio of vertical length to horizontal length;
 n = van Genuchten coefficient of uniformity of pore space;
 Q = outflow rate from numerical model;
 Q_{Charni} = outflow rate from saturated flow model;
 Q_L = outflow rate under linear pressure distribution assumptions;
 Q_{sat} = total flow rate below water table;
 Q_{uns} = total flow rate above water table;
 x = horizontal distance;
 z = vertical distance;
 $\alpha = \alpha^* L_z$ = ratio of vertical length to height of capillary fringe;
 α^* = van Genuchten (1980) parameter;
 ξ = total head; and
 ψ = pressure head.